PERGAMON

International Journal of Heat and Mass Transfer 43 (2000) 2365–2374

International Journal of HEAT and MASS TRANSFER

www.elsevier.com/locate/ijhmt

Influence of imposed oscillatory frequency on mass transfer enhancement of grooved channels for pulsatile flow

Tatsuo Nishimura*, Naoki Oka, Yoshimichi Yoshinaka, Koji Kunitsugu

Department of Mechanical Engineering, Yamaguchi University, Ube 755-8611, Japan

Received 22 May 1999; received in revised form 20 August 1999

Abstract

The present experimental study describes mass transfer enhancement in grooved channels with different cavity lengths for pulsatile flow. Overall and local mass transfer rates were measured by the electrochemical method with a high Schmidt number and also the vortical motion within the groove was visualized by the electrolytic precipitation method. We especially focused on the influence of oscillation frequency on mass transport enhancement. Transport enhancement by means of fluid oscillation is found to be higher in laminar flow than in turbulent flow. There is a noticeable enhancement at intermediate Strouhal numbers, depending on the cavity length and the net flow Reynolds number. It is revealed that the mechanism for a peak transport enhancement factor against Strouhal number is not explained by the hydrodynamic resonance proposed by Patera and Mikic, under a certain condition.

Keywords: Mass transfer enhancement; Pulsatile flow; Grooved channel; Electrochemical method; Hydrodynamic resonance

1. Introduction

There have been several studies on heat and mass transfer in grooved channels, which are applied to compact heat exchangers, mass transfer devices and electronics cooling under laminar flow conditions. For steady flow, experimental and numerical studies [1–5] show that as flow separates, a periodic redevelopment of the thermal or compositional boundary layer occurs from each rib and its contribution is the most significant part of the total heat or mass transfer rate. However, inside the grooves the heat or mass transfer rate is very small, reducing thus the enhancement of transport rates.

This paper deals with mass transfer enhancement in grooved channels under pulsatile flow conditions. The use of forced time-periodic flow is effective for transport enhancement in systems with separated flow [6–15], especially. Nishimura and Matsune [14] studied experimentally mass transfer with a high Schmidt number in symmetric and asymmetric wavy-walled channels for pulsatile flow. They showed that the enhancement factor for mass transfer increases with the oscillatory fraction and frequency of the flow rate and that the Sherwood number for pulsatile flow can be expressed in terms of the Sherwood numbers for steady and oscillatory flows. Mackley and Stonestreet [12] also examined heat transfer and energy dissipation for pulsatile liquid flow in a baffled tube in a wide range of several flow parameters. On the other hand,

* Corresponding author. Tel.: +81-836-35-9909; fax: +81-836-35-9926.

E-mail address: tnishumu@mechgw.mech.yamaguchi-u.ac.jp (T. Nishimura).

0017-9310/00/$ - see front matter
PII: S0017-9310(99)00311-7

Nomenclature

a	cavity depth
d	piston diameter
D	molecular diffusivity of the ferricyanide ion
E	enhancement factor for mass transfer = Sh_p/Sh_s
f	oscillatory frequency of piston
f_n	frequency for self-sustained oscillation
H	channel height
L	cavity pitch
L_m	mass transfer length
l	cavity length
k	average mass transfer coefficient
k^*	local mass transfer coefficient
P	oscillatory fraction of the flow rate = Q_o/Q_s
Q_i	instantaneous flow rate
Q_o	peak flow rate of oscillatory component
Q_s	net flow rate
Re_c	critical Reynolds number for self-sustained oscillation in steady flow
Re_s	Reynolds number for steady component
s	stroke of piston
Sc	Schmidt number = ν/D
Sh_p	average Sherwood number for pulsatile flow = kH/D
Sh_p^*	local Sherwood number for pulsatle flow = k^*H/D
Sh_s	average Sherwood number for steady flow
Sh_s^*	local Sherwood number for steady flow
St	Strouhal number for pulsatile flow = $2\pi fH/u_s$
St_n	Strouhal number for self-sustained oscillation = $2\pi f_n H/u_s$
T	period of oscillation = $1/f$
t	time
u_s	average velocity through the channel = Q_s/HW
W	channel width

Greek symbol

ν	kinematic viscosity

Patera and Mikic [6] and Greiner [7] found numerically and experimentally that small fluid oscillation at the natural frequency of the hydrodynamic instability increases dramatically the amplitude of the instability within a grooved channel, even for Reynolds numbers below the critical value at the onset of self-sustained oscillations, and thus enhances heat transfer. They called this effect resonant transport enhancement. However, they treated only a grooved channel with small cavities. The effect of cavity length has not been considered. More recently, Nishimura et al. [15] studied fluid mixing and mass transfer with a high Schmidt number in grooved channels with different cavity lengths and found that at high Reynolds numbers the mass transfer enhancement factor suddenly increases at a low oscillatory fraction of the flow rate, depending on the oscillatory frequency and the cavity length, in contrast to the cases at low Reynolds numbers. However, the confirmation of hydrodyanamic resonance proposed by Patera and Mikic [6] has not been performed yet.

In the present study, we examine experimentally the influence of the oscillatory frequency on mass transfer enhancement of grooved channels with different cavity lengths.

2. Experimental apparatus and procedure

The experimental apparatus is the same as that used in the previous study [15]. The volumetric flow rate is

$$Q_i = Q_s + Q_o \sin\left(\frac{2\pi t}{T}\right) \tag{1}$$

where Q_s is the net flow, Q_o is the peak flow of fluid oscillation and T is the period of oscillation.

The net flow is provided by a centrifugal pump and the flow rate is determined with a rotameter. The imposed oscillatory flow is generated by a pulsatile pump, driven by a variable speed motor through a Scotch-Yoke mechanism which allows the length of the stroke and frequency of the piston to be changed. The peak flow rate is determined by

$$Q_o = 2\pi sf\left(\frac{\pi d^2}{4}\right) \tag{2}$$

where s, f ($=1/T$) and d are the length of the stroke, frequency and diameter of the piston, respectively. In this experiment, s and f are variable, but d is fixed.

Fig. 1 shows the dimensions of three channels with different cavity lengths. The channel height, channel width, cavity pitch and the cavity depth are fixed (H = 7 mm, W = 80 mm, L = 33 mm and a = 5.6 mm). The length of the cavity l is variable (l/L = 1/3, 1/2 and 2/3: the so-called S-cavity, M-cavity and L-cavity).

Three flow parameters characterize the pulsatile flow: the net flow Reynolds number based on the channel height, the oscillatory fraction of the flow rate and

Strouhal number

$$Re_s = \frac{u_s H}{\nu} \tag{3}$$

$$P = \frac{Q_o}{Q_s} \tag{4}$$

$$St = \frac{2\pi f H}{u_s} \tag{5}$$

where u_s is the average velocity through the channel ($= Q_s/HW$) and ν is the kinematic viscosity of the fluid.

Experiments were carried out in the following ranges of flow parameters: $40 < Re_s < 1400$, $0 < P < 11$ and $0.035 < St < 5.61$. The net flow Reynolds number range belongs to laminar and turbulent flow regimes. The uncertainties in dimensionless parameters are within the limits of a 3% maximum error.

Flow was visualized by means of the aluminum dust method and the electrolytic precipitation method. Perfusion with an aqueous suspension of aluminum particles, about 40 μm in diameter, enabled the observation of the pathlines approximately corresponding to streamlines. The elctrolytic precipitation method was employed to observe the behavior of fluid exchange between the channel and groove parts. Mass transfer rates were measured by the electrochemical method, which can be applied to pulsatile flow [16]. The electrochemical reaction used is the cathodic reduction of ferricyanide ions to ferrocyanide ions at the cathode. Three cathodes of nickel placed in the 5th, 6th and 7th grooves from upstream of the channel were used to determine the effect of length of the mass transfer section on the average mass transfer rates as shown in Fig. 2. Furthermore, the local mass transfer rates along the bottom of the groove were measured. The electrolyte used contained 0.01 N potassium ferriferrocyanide and 1.0 N sodium hydroxide, and its temperature was kept at 25°C by a heat exchanger ($Sc = 1570$). Under the analogy between heat and mass transfer, this system is equivalent to a high Prandtl number heat transfer.

3. Results and discussion

3.1. Steady flow experiment ($P = 0.0$)

In this experimental range, fluid flow under a constant flow rate for the grooved channels changes from a steady to oscillatory state at a critical value of the Reynolds number, smaller than for the grooveless channel. Self-sustained oscillation characteristics in these channels have been described in the previous flow studies [17,18]. The critical Reynolds number for the onset of self-sustained oscillation depends on the cavity length and its value becomes smaller when the cavity length increases, i.e., $Re_c = 300$ for L-cavity, 450 for M-cavity and 1000 for S-cavity. These oscillations correspond to Tollmien–Schlichting traveling waves and the dimensionless natural frequency ($St_n = 1.92$) closely matches that for the grooveless channel flow with the same channel height. Fig. 3 shows mass transfer results for steady flow. The average mass transfer rates measured in the 5th groove are presented in Fig. 3(a) as $Sh_s/Sc^{1/3}$ vs. Re_s. The dependence of the Reynolds number on the Sherwood number increases after the onset of self-sustained oscillation for L-cavity and M-cavity. While, for S-cavity a slight increment of the Reynolds number dependence is identified before the oscillatory flow. The solid line in the figure denotes the mass transfer of the gooveless channel obtained by Leveque theory [19]. At high Reynolds numbers, all of the grooved channels have larger Sherwood numbers than the grooveless channel.

The effect of mass transfer length for S-cavity is shown in Fig. 3(b) as an example. This result indicates

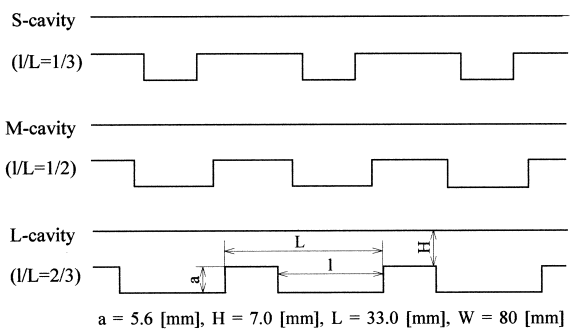

Fig. 1. Details of test section.

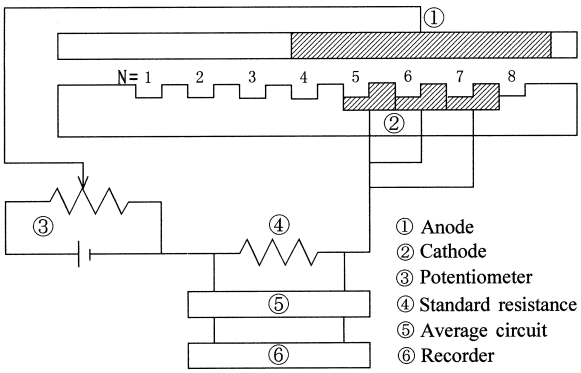

Fig. 2. Positions of electrodes and electrical circuit.

that unlike the grooveless channel, the presence of periodic grooves retards the development of the concentration boundary layer along the lower wall of the channel, although the experimental data are slightly scattered due to the uncertainties of the setting of each electrode used for the mass transfer measurement.

Local Sherwood numbers measured in the 5th groove for S-cavity is shown in Fig. 3(c). The increment of the Sherwood number against the Reynolds number at the rib (electrode D) is not so large even after the onset of self-sustained oscillation ($Re_c = 1000$). On the other hand, the variation of the Sherwood numbers along the bottom of the groove (electrodes A, B and C) with the Reynolds number is complicated, which suggests a remarkable change in the vortical motion within the groove in the Reynolds number range from 100 to 1000, prior to the onset of self-sustained oscillation. Fig. 4 shows flow visualization photographs for three different Reynolds numbers. The electrolytic precipitation method was employed and the smoke of a white metallic compound was electrochemically produced from an electro-conductive paint on the bottom of the groove. The primary vortex and the upstream secondary vortex are clearly visible. It is noticeable that the secondary vortex becomes more significant as the Reynolds number increases, which indicates the breakdown of the concentration boundary layer along the bottom of the groove for a system with high Schmidt number, leading to promotion in the local Sherwood numbers (electrodes A and B) at Reynolds numbers greater than 600 as shown in Fig. 3. Unfortunately, this flow visualization was not discernible at lower Reynolds numbers. However, according to the previous numerical flow analysis [17], the absolute value of the wall shear rate at the upstream part of the groove corresponding to the position of electrode A has a maximum near $Re_s = 150$ due to the occurrence of the secondary vortex, in contrast to that at the downstream part (electrodes B and C). The behavior of the wall shear rate due to the secondary vortex seems to lead to a small reduction of the local Sherwood number for electrode A in the Reynolds number range from 100 to 250. At higher Reynolds numbers, the concentration boundary layer develops from the upstream part due to the secondary vortex growth, which appears to again increase the Sherwood number as shown in Fig. 4. Thus the occurrence of the secondary vortex is found to provide a significant influence on the local mass transfer within the groove even before the onset of self-sustained oscillation, which corresponds to the result of the average mass transfer as shown in Fig. 3(a). The mass transfer characteristics for L-cavity has been reported in reference [20].

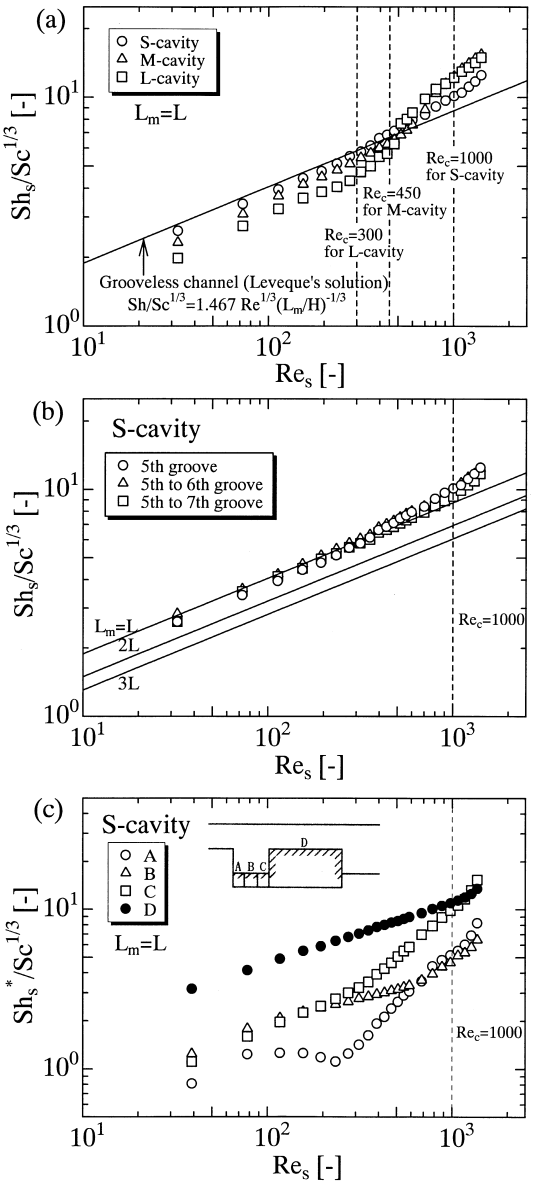

Fig. 3. Sherwood number vs. Reynolds number for steady flow.

3.2. Pulsatile flow experiment ($P > 0.0$)

As mentioned above, the effect of mass transfer length in the grooved channels is insignificant. So we measured the time-averaged mass transfer rates in the 5th groove for pulsatile flow. Sherwood numbers for pulsatile flow are normalized by their respective steady values, defining the mass transfer enhancement factor, $E = Sh_p/Sh_s$. Fig. 5 shows the relationship between the enhancement factor and the oscillatory fraction of the

flow rate at three Reynolds numbers. At $Re_s = 56$ as shown in Fig. 5(a), as the oscillatory fraction P increases, the enhancement factor E becomes increasingly larger than unity and its value hardly depends on the Strouhal numbers St for each cavity. The reason for this is not evident at the present time although the flow patterns strongly depend on the oscillation frequency as discovered by the previous flow analysis [21]. Similar experimental results for transport enhancement have been obtained in other wavy-walled channels [13,14]. The dotted line in each figure denotes a referential line, with no physical meaning, drawn only to compare the enhancement factors for different cavity lengths. The enhancement factor tends to increase as the cavity length becomes large. On the other hand, at $Re_s = 692$ as shown in Fig. 5(b), the effect of Strouhal number is remarkable, although depending on the cavity length. That is, the enhancement factor increases with decreasing Strouhal number in this experimental range. Unfortunately, the presence

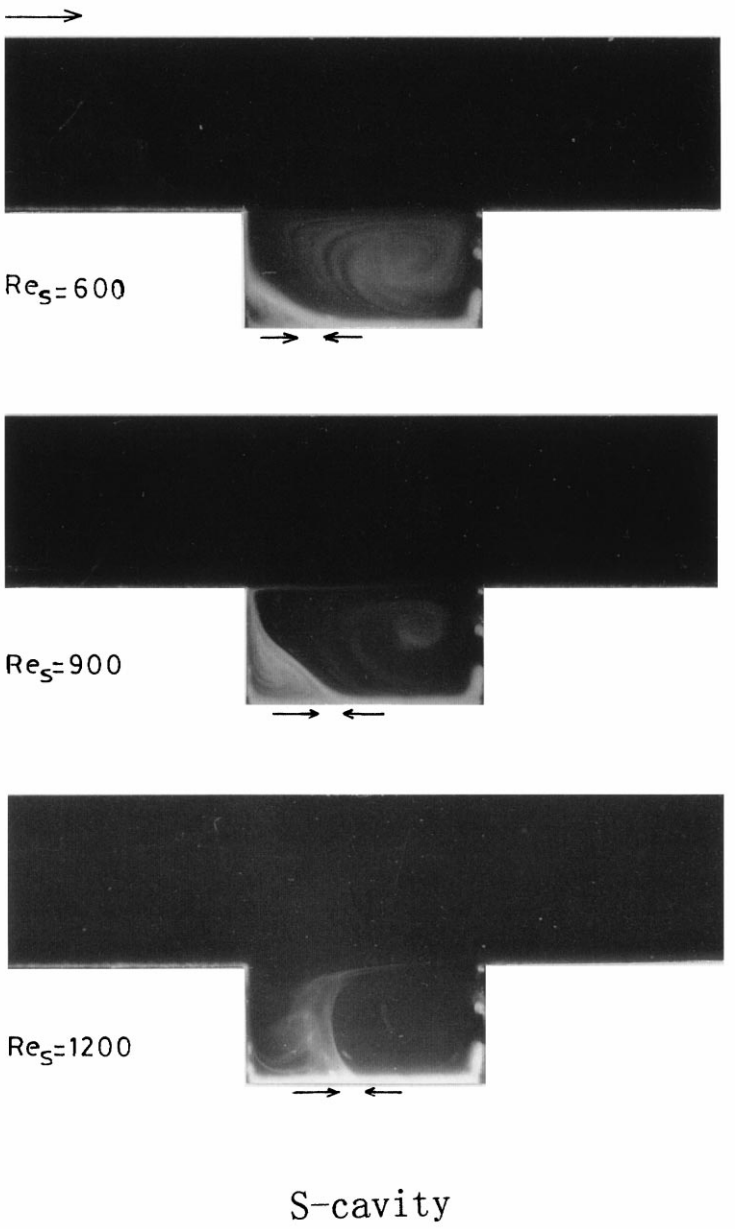

Fig. 4. Flow visualizations for steady flow.

of resonant transport enhancement at this Reynolds number is not evident, because the Strouhal number range is below the dimensionless natural frequency $St_n = 1.92$ mentioned in the steady flow experiment, due to limitations of the pulsatile pump. Also, the enhancement factor of M-cavity has a large value, relative to those for other cavities. However, with a further increase of the Reynolds number (see Fig. 5(c)), the enhancement factor for S-cavity tends to have a large value, although the effect of Strouhal number remains the same. The reason for this is that the critical Reynolds number for S-cavity is considerably larger than those for other cavities as mentioned in the steady flow experiment. It seems that an optimum Reynolds number for maximum enhancement is in the neighbourhood of the critical Reynolds number for each cavity. Similar results have been experimentally obtained for the mass transfer in a furrowed channel with arc-shaped walls [13]. Furthermore, Valencia [22] studied numerically the effect of pulsating inlet of turbulent air flow and heat transfer past a backward-facing step and found that the pulsatility of the inlet flow does not

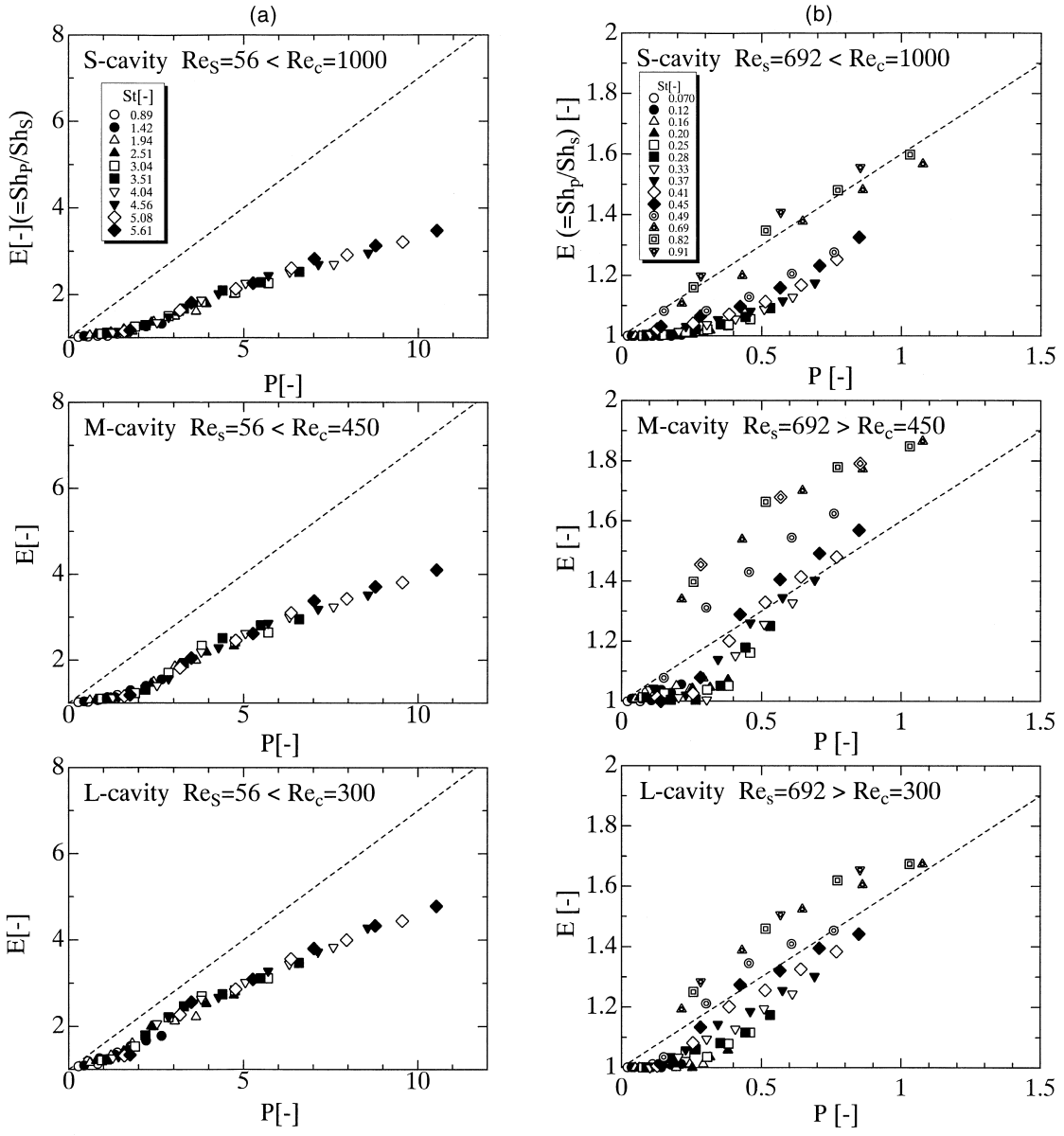

Fig. 5. Enhancement factor vs. oscillatory fraction of the flow rate for different Reynolds numbers.

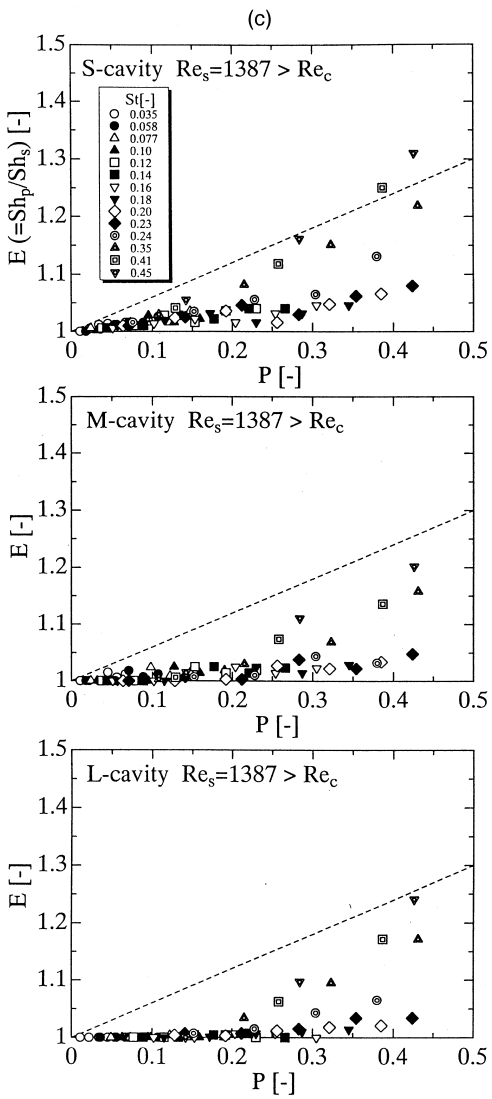

Fig. 5 (*continued*)

impact the heat transfer. Thus we conclude that the transport enhancement by means of fluid oscillation is higher in laminar flow than in turbulent flow, which is important from practical applications. The use of pulsatile flow is effective to the design of electrysers and membrane bioreactors operated at low Reynolds numbers. Furthermore, if the optimum fluid-mechanical conditions for mass transfer are considered in terms of the energy efficiency of a pulsatiling pumping system, the increase in power dissipation has to be reduced.

In Fig. 5, resonant transport enhancement proposed by Patera and Mikic [6] is not confirmed. So we examined this transport enhancement under a certain condition. Fig. 6 shows the relationship between the enhancement factor and the Strouhal number for different cavity lengths at two Reynolds numbers. The oscillatory fraction of the flow rate, P is less than unity and it is set close to 0.4. The enhancement factor increases with Strouhal number, but tends to decrease above a certain Strouhal number. The features depend on the cavity length and the Reynolds number. That is, the enhancement factor increases at $Re_s = 234$ and 500 as the cavity length becomes large. According to hydrodynamic resonance, it is expected that a peak of the enhancement factor appears near the Strouhal number corresponding to self-sustained oscillation for steady flow, i.e., $St_n = 1.92$. The trend is different between $Re_s = 234$ and 500. That is, at $Re_s = 500$, the peak value of the enhancement factor appears near the Strouhal number of self-sustained oscillation for each cavity. While, at $Re_s = 234$, the feature for L-cavity is quite different from those for M-cavity and S-cavity, i.e., no sharp peak is observed and there is a plateau in the Strouhal number range from 0.4 to 1.3. So we measured local enhancement factors for $Re_s = 234$ and $P = 0.43$. As shown in Fig. 7, there is no substantial enhancement at the rib (elecrode D) for both S-cavity and L-cavity. On the other hand, the local enhancement factors along the bottom of the groove (electrodes A, B and C) strongly depend on the Strouhal number and the cavity length. In particular, the enhancement factor at the upstream part (electrode A) is greatly affected. For S-cavity, the maximum value appears near $St = St_n$, while for L-cavity, it occurs at a smaller Strouhal number than the value of St_n. Thus it is revealed that the Strouhal number for a maximum transport enhancement does not correspond to the dimensionless natural frequency, for L-cavity under a certain condition, in contrast to S-cavity, and it seems that the vortical structures within the groove are quite different between S-cavity and L-cavity.

As shown in the previous study [15], a comparison between the aluminum dust method, from an Eulerian view, and the electrolytic precipitation method, from a Lagrangian perspective, demonstrates that the combined effect of the separated vortex and fluid oscillation promotes the exchange of fluid between the channel and groove parts, leading to mass transfer enhancement along the bottom of the groove as shown in Fig. 7. In particular, the ejection of fluid within the groove into the mainstream at the moment of $t/T = 0.0$ is observed. The effect of Strouhal number for both cavities at $Re_s = 234$ and $P = 0.43$ is shown in Fig. 8. As the Strouhal number increases, the ejection of fluid within the groove for S-cavity is gradually promoted. In other words, the smoke of a white metallic compound produced from the bottom of the groove does not persist within the groove. However, above a certain value of Strouhal number, the ejection is

reduced (see the result at $St = 3.43$). While, the fluid ejection process for, L-cavity is more complicated in the upstream part of the groove than that for S-cavity, and also a larger amount of fluid is ejected even at lower Strouhal numbers than the value of St_n. However, it should be noted that at high Strouhal numbers, the ejection process becomes identical for both cavities, indicating the reduction in fluid ejection. The reason for this may be due to viscous effects at high oscillatory frequencies indicated in the previous numerical flow analysis [2]. These flow visualization results correspond well to the behavior of transport enhancement as shown in Figs. 6 and 7.

At higher Reynolds numbers, the electrolytic precipitation method is not applicable, because the smoke produced from the electro-conductive paint rapidly diffuses. Flow visualization photographs by the combination of aluminum dust method and electrolytic precipitation method indicate that the fluid exchange between the channel and groove parts is more significant with increasing the Strouhal number and the flow seems to include turbulence, but not shown here due to limitations of the space.

Thus we confirm that there is a substantial enhancement at intermediate Strouhal numbers, depending on the cavity length and the Reynolds number. The mechanism for a peak transport ehnancement against Strouhal number is not explained by only the hydrodynamic resonance proposed by Mikic and Patera [6], under a certain condition. Although the reason for this is not evident at the present time, one possible cause of the effect of Strouhal number on transport enhancement is related to Kelvin–Helmholtz instability, in addition to Tollmien–Schlichting instablity for pulsatile flow. Because the separated shear layer above the groove is likely to grow up for a large cavity length. More recently, the present authors [23] performed numerical flow analysis for L-cavity and S-cavity under the same fluid mechanical conditions and discovered a significant oscillatory shear stress due to the contribution of the oscillating components in velocity, near $St = 0.8$

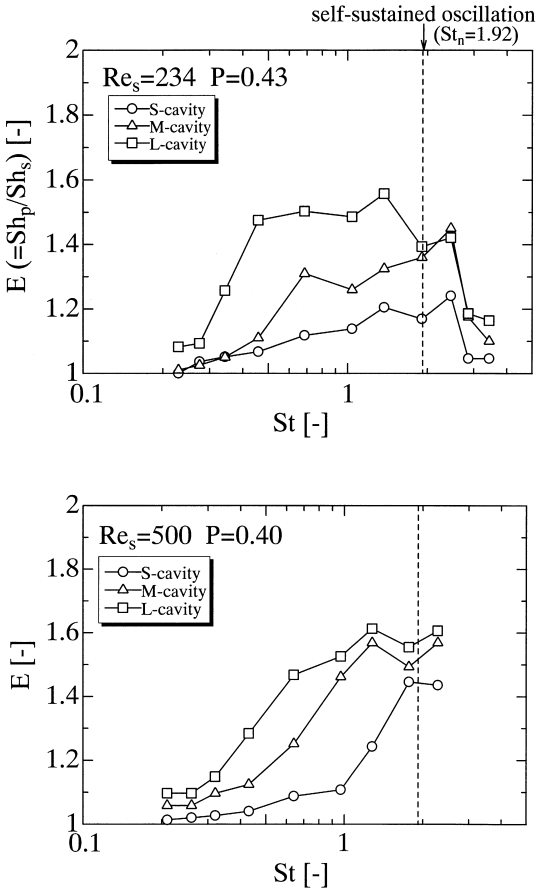

Fig. 6. Enhancement factor vs. Strouhal number for different Reynolds numbers.

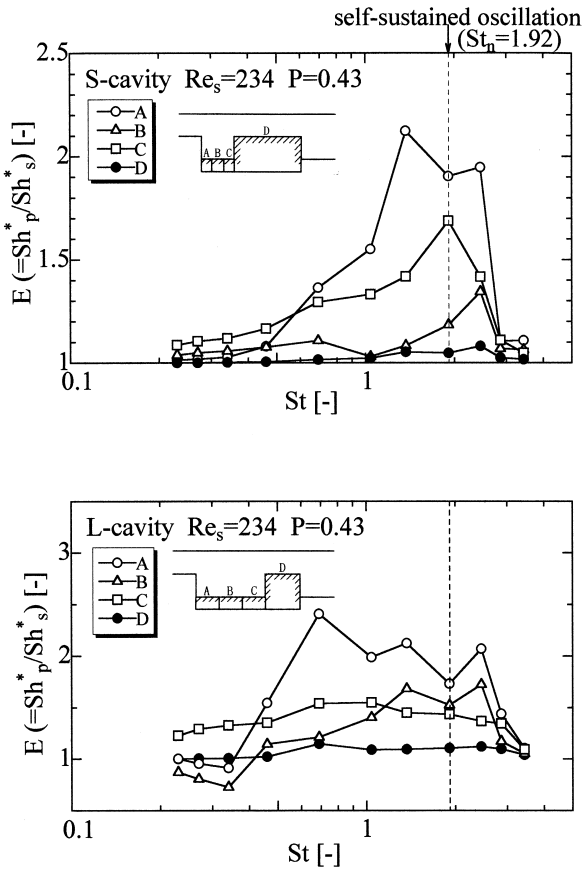

Fig. 7. Local enhancement factor vs. Strouhal number for S-cavity and L-cavity.

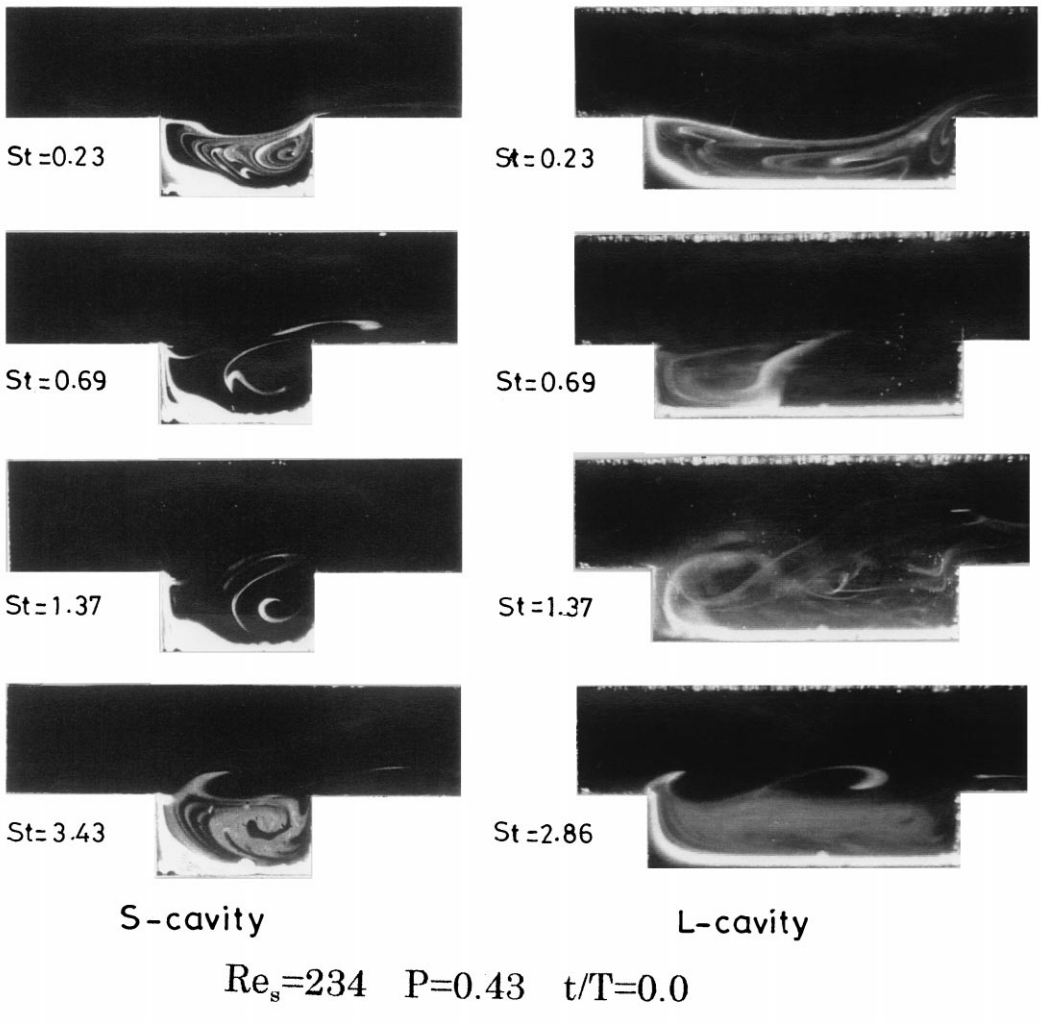

Fig. 8. Effect of Strouhal number on fluid exchange at $Re_s = 234$. $P = 0.43$ for S-cavity and L-cavity.

for L-cavity, unlike the case of S-cavity. Also Chun and Sung [24] found experimentally that the shear layer structure for laminar separation over a backward-facing step is significantly altered at a certain frequency of forced perturbations. Further understanding of physical processes of transport enhancement for different cavity lengths is needed.

4. Conclusions

The experimental study of mass transfer with a high Schmidt number in grooved channels for pulsatile flow has been performed in a wide range of flow parameters. We especially focused on the influence of oscillatory frequency on mass transport enhancement. The following conclusive remarks were drawn:

1. Mass transfer enhancement by means of fluid oscillation is higher in laminar flow than in turbulent flow. There is no substantial enhancement at the rib, whereas it is remarkable at the bottom of the groove.
2. There is a noticiable enhancement at intermediate Strouhal numbers, depending on the cavity length and Reynolds number. The mechanism for a peak transport enhancement factor against Strouhal number is not explained by only the hydrodynamic resonance proposed by Patera and Mikic [6], under a certain condition. This is subject of a future work.

Acknowledgements

This work was supported in part by a Grant-in-Aid for Science Research (Nos. 06650208 and 09750196) from the Ministry of Education, Science and Culture of Japan. The authors acknowledge with thanks the assistance of graduate student Fawzi bin Ahmad in the experiments.

References

[1] B. Farhanieh, C. Herman, B. Sunden, Numerical enhancement and experimental analysis of laminar fluid flow and forced convection heat transfer in a grooved duct, Int. J. Heat Mass Transfer 36 (1993) 1609–1617.
[2] T. Fusegi, Numerical study of mixed convection in a channel with periodic cavities, Proc. of 9th Int. Heat Transfer Conf. 5, 1994, pp. 471–476.
[3] J.S. Nigen, C.H. Amon, Time-dependent conjugate heat transfer characteristics of self-sustained oscillatory flows in a grooved channel, ASME J. Fluid Eng 116 (1994) 499–507.
[4] C. Herman, E. Kang, H. Huang, B. Puranik, Experimental visualization of unsteady temperature fields in electronic cooling applications, ASME HTD vol. 319/EEP-vol. 15 (1995) 33–40.
[5] T. Nishimura, K. Kunitsugu, H. Nakagiri, Fluid mixing and local mass transfer characteristics in a grooved channel for self-sustained oscillatory flow, Heat Transfer Jpn Res 27 (1998) 522–534.
[6] A.T. Patera, B.B. Mikic, Exploiting hydrodynamic instabilities, resonant heat transfer enhancement, Int. J. Heat Mass Transfer 29 (1986) 1127–1138.
[7] T. Nishimura, A. Tarumoto, Y. Kawamura, Flow and mass transfer characteristics in wavy channels for oscillatory flow, Int. J. Heat Mass Transfer 30 (1987) 1007–1015.
[8] M. Greiner, An experimental investigation of resonant heat transfer enhancement in grooved channels, Int. J. Heat Mass Transfer 34 (1991) 1381–1391.
[9] T. Nishimura, S. Murakami, Y. Kawamura, Mass transfer in a symmetric sinusoidal wavy-walled channel for oscillatory flow, Chem. Eng., Sci 48 (1993) 1793–1800.
[10] T. Nishimura, Heat and mass transfer enhancement by chaotic mixing in laminar flow, Trends in Chem. Eng 2 (1994) 199–214.
[11] T. Nishimura, N. Kojima, Mass transfer enhancement in a symmetric sinusoidal wavy-walled channel for pulsatile flow, Int. J. Heat Mass Transfer 38 (1995) 1719–1731.
[12] M.R. Mackley, P. Stonestreet, Heat transfer and associated energy dissipation for oscillatory flow in baffled tubes, Chem. Eng. Sci 50 (1995) 2211–2224.
[13] T. Nishimura, Mass transfer enhancement in a furrowed channel with arc-shaped walls for pulsatile flow, Heat Transfer Jpn. Res 24 (1995) 115–132.
[14] T. Nishimura, S. Matsune, Mass transfer enhancement in a sinusoidal wavy channel for pulsatile flow, Heat and Mass Transfer 32 (1996) 65–72.
[15] T. Nishimura, K. Kunitsugu, A.M. Morega, Fluid mixing and mass transfer enhancement in grooved channels for pulsatile flow, J. Enhanced Heat Transfer 5 (1998) 23–37.
[16] T. Mizushina, The electrochemical method in transport phenomena, in: T.P. Irvine, J.P. Hartnettt (Eds.), Advances in Heat Transfer, vol. 7, Academic Press, New York, 1971, pp. 87–181.
[17] T. Nishimura, H. Nakagiri, K. Kunitsugu, Flow patterns and wall shear stresses in grooved channels at intermediate Reynolds numbers — effect of groove length, Trans JSME Ser. B 62 (1996) 2106–2112.
[18] T. Nishimura, K. Kunitsugu, Self-sustained oscillatory flow and fluid mixing in grooved channel, Kagaku Kogaku Ronbunshu 23 (1997) 764–771.
[19] M.A. Leveque, Leveque Leslois de la transmission de chaleur par convection, Annus Mines Ser 12 (13) (1928) 234–242.
[20] T. Nishimura, K. Kunitsugu, H. Nakagiri, Mass transfer characteristics in a grooved channel for self-sustained oscillatory flow, in: M. Giot, F. Maynger, G.P. Celata (Eds.), Proc. of 4th World Congress of Exp. Heat Transfer, Fluid Mech. and Thermodynamics, 1997, pp. 1963–1970.
[21] T. Nishimura, A.M. Morega, K. Kunitsugu, Vortex structure and fluid mixing in pulsatile flow through periodically grooved channels at low Reynolds numbers, JSME Int. J. Ser B40 (1997) 377–385.
[22] A. Valencia, Effect of pulsating inlet on the turbulent flow and heat transfer past a backward-facing step, Int. Comm. Heat Mass Transfer 243 (1997) 1009–1018.
[23] T. Nishimura, Y. Yoshinaka, K. Kunitsugu, Flow pattern and oscillatory momentum transport in grooved channels for pulsatile flow, Proc. of Annual Meeting of JSME 4, 1999, pp. 3–4.
[24] K.B. Chun, H.J. Sung, Visualization of a locally-forced separated flow over a backward-facing step, Exp. Fluids 25 (1998) 133–142.